

Technical report 15-020

Model predictive control for freeway networks based on multi-class traffic flow and emission models*

S. Liu, H. Hellendoorn, and B. De Schutter

August 2015

Submitted to a journal.

Delft Center for Systems and Control
Delft University of Technology
Mekelweg 2, 2628 CD Delft
The Netherlands
phone: +31-15-278.51.19 (secretary)
fax: +31-15-278.66.79
URL: <http://www.dcsc.tudelft.nl>

*See http://pub.deschutter.info/abs/15_020.html for up-to-date information on this report.

Model Predictive Control for Freeway Networks Based on Multi-Class Traffic Flow and Emission Models

Shuai Liu, Hans Hellendoorn, and Bart De Schutter

Abstract—In this paper we develop and investigate some multi-class macroscopic traffic flow and emission models: a new multi-class METANET model, and two new emissions models: multi-class VT-macro and multi-class VERSIT+. To allow comparison with the new multi-class METANET model, we also extend the first-order multi-class traffic flow model FASTLANE with variable speed limits and ramp metering. These new multi-class macroscopic traffic flow and emission models are used as prediction models in online model predictive control for freeway networks. Besides, end-point penalties are also included to account the future extension of the traffic systems beyond the prediction horizon. A simulation experiment is implemented to evaluate the multi-class models. The results show that the approaches based on multi-class METANET and the developed emission models (multi-class VT-macro or multi-class VERSIT+) can improve the performance for total time spent and total emissions w.r.t. the non-control case, and they are more capable of dealing with the queue length constraints than the approaches based on FASTLANE for the setting in our experiment. Including end-point penalties can further improve the performance for the approaches based on multi-class METANET, but not for the approaches based on FASTLANE, probably due to the less reliable estimations of end-point penalties.

I. INTRODUCTION

Traffic management can be used to prevent traffic congestion and to reduce traffic emissions and fuel consumption. There are many ways to realize traffic management. Online model-based control is a popular approach in literature [1–5], and it can provide satisfying performance since it takes the predicted future evolution of traffic flows into account. In this kind of control approach, traffic models are necessary to describe the evolution of traffic states. Hence, appropriate traffic models are important for efficient online model-based traffic control. Many traffic models have been developed for describing traffic flows, emissions, and fuel consumption. In general, microscopic models are more accurate than macroscopic models because they describe the states of individual vehicles. However, this also implies that microscopic models are often time-consuming when simulating large-scale networks. In order to reduce the computation load, macroscopic traffic models are often used in online model-based traffic control. Many macroscopic models are homogeneous, and this means that the differences among different kinds of vehicles are

neglected. Real traffic networks subsume various types of vehicles, such as cars, vans, trucks, etc. This leads to the need of macroscopic models that can describe the heterogenous nature of real traffic networks. These models are called multi-class traffic models. Many performance indicators can be adopted in traffic management, such as total time spent, total emissions, and total fuel consumption. Therefore, both traffic flow models and emission and fuel consumption models are needed for traffic management aiming at the above-mentioned performance indicators.

Several multi-class macroscopic traffic flow models have been developed. Wong and Wong [6] extended the Lighthill-Whitham-Richards (LWR) model [7, 8] to a multi-class version, in which the essential characteristics of each vehicle class remain unchanged. More specifically, the states of each vehicle class are calculated through its own fundamental diagram by using the total density. Logghe [9] also developed a multi-class version of the LWR model, where each class is subject to its own fundamental diagram, and is limited within an assigned space of the road. Van Lint et al. [10] proposed the FASTLANE model, which is a first-order multi-class macroscopic model. Here dynamic passenger car equivalents are used to describe different vehicle classes, taking into account the differences in the space occupied by a vehicle class under different traffic conditions (e.g. different densities). Caligaris et al. [1] extended the macroscopic model described in [11] by accounting for two different vehicle classes. They used the steady-state relation between speed and density for representing the interference between these two vehicle classes they used. Deo et al. [12] proposed a multi-class version of the METANET model [13, 14] in which passenger car equivalents are used to represent different vehicle classes. Here the desired speed of each vehicle class is computed through a convex combination of the desired speeds of all vehicle classes, which reduces the heterogeneity of this model. The METANET model is a second-order model, which is in general more accurate than a first-order model. This is due to the fact that second-order models can capture phenomena that cannot be described by first-order models [15–17], such as FASTLANE. In addition, the METANET model can reproduce capacity drop near on-ramps and in shock waves; this is very important for online model-based traffic control [16]. Note, however, that a second-order model in general makes the computation more complex than a first-order model. Hence, a trade-off between

computation complexity and accuracy should be considered for online model-based control.

Traffic emission and fuel consumption models are necessary for the reduction of traffic emissions and fuel consumption in online model-based traffic control. Many microscopic emission and fuel consumption models have been developed for describing the emissions and fuel consumption of individual vehicles. These emission and fuel consumption models can be classified according to their inputs. Some emission and fuel consumption models use the vehicle speed as input, such as COPERT [18, 19] and PHEM [20]. However, other emission and fuel consumption models use both the speed and the acceleration as inputs, e.g. VT-micro [21], VERSIT+ [22, 23]. For online model-based control, macroscopic models are needed for reducing the computation load. Csikos et al. [3] extended the COPERT model into a macroscopic version by introducing the concept of the spatiotemporal window. Zegeye et al. [4] developed the VT-macro model by integrating the VT-micro model with METANET. In comparison with the macroscopic version of the COPERT model, the VT-macro model does not only use the speed but also the acceleration as input. However, the VT-macro model is still homogeneous, i.e., all vehicles are assumed to have the same physical characteristics. When the VT-macro model is applied in a multi-class setting, a multi-class version needs to be developed, which will also be done in this paper.

The contributions of this paper are as follows.

- A new multi-class METANET model: Inspired by the approach used for deriving a multi-class version of the LWR model [9], we develop a new multi-class METANET model. In order to obtain more heterogeneity, desired speeds are computed in a different way than the multi-class METANET developed by Deo et al. [12].
- Extensions of FASTLANE: For applying FASTLANE in Model Predictive Control (MPC) for traffic network, we incorporate ramp metering and variable speed limit in FASTLANE.
- Extensions of VT-macro model to be multi-class: We extend the VT-macro model into a multi-class version, so that it can be used in a multi-class setting.
- A multi-class VERSIT+ model: Since we intend to use the VERSIT+ model together with multi-class macroscopic traffic flow models, we will develop a multi-class macroscopic version of this model. Considering that jerk (the derivative of acceleration) is also one of the measurements [24], extending the VERSIT+ model by including jerk as an input is also possible.
- End-point penalties: We propose to include end-point penalties in the objective function, so that the differences among vehicles that are at different positions can be captured.

For investigating these multi-class macroscopic traffic models, we apply them in an online model-based traffic control system. MPC is used as the control approach,

considering that it can deal with nonlinear systems, multi-criteria optimization, and constraints. The Total Time Spent (TTS) and the Total Emissions (TE) are both included in the objective function of the online model-based traffic control, since we want to achieve a balanced trade-off between these two performance indicators.

This paper is organized as follows. In Section II, we present the relevant traffic models METANET and FASTLANE. In Section III, we introduce the relevant emission models VT-macro and VERSIT+. Next we develop multi-class METANET, and extend FASTLANE with speed limits and ramp metering in Section IV. We also develop new emission models: multi-class VT-macro and multi-class VERSIT+ in Section V. In Section VI, we develop online MPC for freeway traffic networks. After that, a simulation experiment is implemented in Section VII to compare the efficiency of the proposed multi-class macroscopic traffic models for model-based online traffic control.

II. TRAFFIC FLOW MODELS

A. METANET

The METANET model [13, 14] is a second-order macroscopic model that describes traffic networks with uniform links corresponding to freeway stretches. Nodes are used to represent on-ramps, off-ramps, or other changes in geometry. Each link is divided into several homogenous segments, which are similar with the concept of cells in FASTLANE. These segments are characterized by segmental variables: traffic density ($\rho_{m,i}(k)$), space mean speed ($v_{m,i}(k)$), and outflow ($q_{m,i}(k)$) in segment i of link m at time step k . The evolution of these variables is described through the following equations

$$q_{m,i}(k) = \mu_m \rho_{m,i}(k) v_{m,i}(k) \quad (1)$$

$$\rho_{m,i}(k+1) = \rho_{m,i}(k) + \frac{T}{L_m \mu_m} (q_{m,i-1}(k) - q_{m,i}(k)) \quad (2)$$

$$v_{m,i}(k+1) = v_{m,i}(k) + \frac{T}{\tau} (V(\rho_{m,i}(k)) - v_{m,i}(k)) + \frac{T}{L_m} v_{m,i}(k) (v_{m,i-1}(k) - v_{m,i}(k)) - \frac{T \eta}{L_m \tau} \frac{\rho_{m,i+1}(k) - \rho_{m,i}(k)}{\rho_{m,i}(k) + \kappa} \quad (3)$$

$$V(\rho_{m,i}(k)) = v_{\text{free},m} \exp \left[-\frac{1}{a_m} \left(\frac{\rho_{m,i}(k)}{\rho_{\text{crit},m}} \right)^{a_m} \right] \quad (4)$$

where $V(\rho)$ is the desired speed at density ρ , $v_{\text{free},m}$ is the free flow speed of link m , $\rho_{\text{crit},m}$ is the critical density of link m , and τ , η , κ , and a_m are model parameters. Node equations that describe flows between adjacent segments can be found in [25].

A variable speed limit can be included by modifying the desired speed expression. According to Hegyi et al. [25], one

way to incorporate a variable speed limit is

$$V(\rho_{m,i}(k)) = \min \left(v_{\text{free},m} \exp \left[-\frac{1}{a_m} \left(\frac{\rho_{m,i}(k)}{\rho_{\text{crit},m}} \right)^{a_m} \right], \right. \\ \left. (1 + \delta_m) v_{\text{SL},m,i}(k) \right) \quad (5)$$

where $v_{\text{SL},m,i}$ is the speed limit that is applied in segment i of link m , and $1 + \delta_m$ is the non-compliance factor of link m , which allows for modeling enforced and unenforced variable speed limits.

Besides, the lengths of the queues at mainstream origins and on-ramp origins are described by

$$w_o(k+1) = w_o(k) + T(d_o(k) - q_o(k)) \quad (6)$$

where w_o is the queue length at origin o , d_o is the demand at origin o , and q_o is outflow at origin o .

For a mainstream origin, the outflow is

$$q_o(k) = \min \left[d_o(k) + \frac{w_o(k)}{T}, q_{\text{lim},m,1}(k) \right] \quad (7)$$

where $q_{\text{lim},m,1}$ is the maximal inflow of the first segment of link m that is connected to the origin:

$$q_{\text{lim},m,1}(k) = \begin{cases} \mu_m \rho_{\text{crit},m} v_{\text{lim},m,1}(k) \left[-a_m \ln \left(\frac{v_{\text{lim},m,1}(k)}{v_{\text{free},m}} \right) \right]^{\frac{1}{a_m}}, & \text{if } v_{\text{lim},m,1}(k) < V(\rho_{\text{crit},m}) \\ \mu_m \rho_{\text{crit},m} V(\rho_{\text{crit},m}), & \text{if } v_{\text{lim},m,1}(k) \geq V(\rho_{\text{crit},m}) \end{cases} \quad (8)$$

where $v_{\text{lim},m,1}(k) = \min(v_{\text{control},m,1}(k), v_{m,1}(k))$ is the speed that limits the flow, with $v_{\text{control},m,1}$ the speed limit of segment $(m, 1)$.

For an on-ramp origin, the outflow is determined by:

$$q_o(k) = \min \left[d_o(k) + \frac{w_o(k)}{T}, C_o r_o(k), C_o \left(\frac{\rho_{\text{max},m} - \rho_{m,1}(k)}{\rho_{\text{max},m} - \rho_{\text{crit},m}} \right) \right] \quad (9)$$

where C_o is the capacity of on-ramp o , $(m, 1)$ is the index of the segment that the on-ramp is connected to, and $\rho_{\text{max},m}$ is the maximum density of link m . For more details about METANET and its extensions, we refer to [13], [14] and [25].

B. FASTLANE

FASTLANE [26, 27] is a first-order multi-class traffic flow model that is represented by links (indexed by m), where each link is divided into several homogeneous cells (indexed by i). In the ensuing, the index c is used to denote vehicle classes. Here we give the discrete-time form of the FASTLANE model, since we use it within a MPC framework in this paper.

FASTLANE is a multi-class version of the LWR model. The main feature of FASTLANE is that it uses dynamic passenger car equivalents (pce) to transform different vehicle classes to a representative vehicle class. The different space occupied by vehicles under different traffic conditions

(different traffic densities) is taken into account in the dynamic pce. In FASTLANE, the dynamic pce ($\eta_{m,i,c}$) value is defined as

$$\eta_{m,i,c} = \frac{s_c + T_{h,c} \cdot v_{m,i,c}}{s_1 + T_{h,1} \cdot v_{m,i,1}} \quad (10)$$

in which $v_{m,i,c}$ is the speed of vehicles of class c in cell i of link m , s_c is the class-specific gross stopping distance of vehicles of class c , and $T_{h,c}$ is the class-specific minimum time headway of vehicles of class c . The index 1 denotes the reference class.

Based on dynamic pce, the effective density¹ ($\rho_{m,i}^{\text{efc}}$) in cell i of link m is defined as

$$\rho_{m,i}^{\text{efc}} = \sum_{c=1}^{n_c} \eta_{m,i,c} \rho_{m,i,c} \quad (11)$$

where $\rho_{m,i,c}$ is the density¹ of vehicles of class c in cell i of link m , and n_c is the number of vehicle classes.

Since we use MPC in this paper, the discrete-time form of (11) is given as follows:

$$\rho_{m,i}^{\text{efc}}(k) = \sum_{c=1}^{n_c} \eta_{m,i,c}(k-1) \rho_{m,i,c}(k) \quad (12)$$

where k is the time step counter, which corresponds to the time instant $t = kT$.

The basic equations for computing flow, density, and speed are

$$q_{m,i,c}(k) = \mu_m \rho_{m,i,c}(k) v_{m,i,c}(k) \quad (13)$$

$$\rho_{m,i,c}(k+1) = \rho_{m,i,c}(k) + \frac{T}{L_m \mu_m} \left(q_{m,c}^{i-1,i}(k) - q_{m,c}^{i,i+1}(k) \right) \quad (14)$$

$$v_{m,i,c}(k) = V_c(\rho_{m,i}^{\text{efc}}(k))$$

$$= \begin{cases} v_{m,c}^{\text{free}} - \rho_{m,i}^{\text{efc}}(k) \frac{(v_{m,c}^{\text{free}} - v_{m,c}^{\text{crit}})}{\rho_{m,i}^{\text{crit}}} & \text{for } \rho_{m,i}^{\text{efc}}(k) < \rho_{m,i}^{\text{crit}} \\ \frac{v_{m,c}^{\text{crit}} \rho_{m,i}^{\text{crit}}}{\rho_{m,i}^{\text{efc}}(k)} \left(1 - \frac{\rho_{m,i}^{\text{efc}}(k) - \rho_{m,i}^{\text{crit}}}{\rho_{m,i}^{\text{max}} - \rho_{m,i}^{\text{crit}}} \right) & \text{for } \rho_{m,i}^{\text{efc}}(k) \geq \rho_{m,i}^{\text{crit}} \end{cases} \quad (15)$$

where $q_{m,i,c}$ is the flow of vehicles of class c in cell i of link m , $q_{m,c}^{i,i+1}$ is the flow of vehicles of class c from cell i to cell $i+1$, $v_{m,c}^{\text{free}}$ is the free flow speed of vehicles of class c in link m , $v_{m,c}^{\text{crit}}$ is the joint critical speed for all vehicle classes, $\rho_{m,i}^{\text{crit}}$ is the joint critical density¹ for all vehicle classes, $\rho_{m,i}^{\text{max}}$ is the effective maximum density¹ in link m , μ_m is the number of lanes of link m , T is the simulation time interval, and L_m is the cell length, satisfying the constraint $\frac{T}{L_m} \geq \max_{c=1,\dots,n_c} \{v_{m,c}^{\text{free}}\}$.

The traffic demand of cell i needs to be distributed among different vehicle classes, according to the traffic composition of cell i . This composition is represented by the flow ratio $\lambda_{m,i,c}$:

$$\lambda_{m,i,c}(k) = \frac{\eta_{m,i,c}(k) q_{m,i,c}(k)}{\sum_{c=1}^{n_c} \eta_{m,i,c}(k) q_{m,i,c}(k)} \quad (16)$$

¹The effective density $\rho_{m,i}^{\text{efc}}$, the critical density $\rho_{m,i}^{\text{crit}}$, and the effective maximum density $\rho_{m,i}^{\text{max}}$ are in pce/km/lane, the density of vehicles of class c in cell i of link m is in vehicle/km/lane.

The class-specific flow from cell i to $i+1$ is described as follows:

$$q_{m,c}^{i,i+1}(k) = \frac{1}{\eta_{m,i,c}(k)} \min \left(D_{m,i,c}(k), \lambda_{m,i,c}(k) S_{m,i+1}(k) \right) \quad (17)$$

where the demand $D_{m,i,c}$ and supply $S_{m,i}$ are defined as

$$D_{m,i,c}(\rho_{m,i}^{\text{efc}}(k)) = \begin{cases} \mu_m \eta_{m,i,c}(k-1) \rho_{m,i,c}(k) V_c(\rho_{m,i}^{\text{efc}}(k)) & \text{for } \rho_{m,i}^{\text{efc}}(k) < \rho_m^{\text{crit}} \\ \mu_m \lambda_{m,i,c}(k) \rho_m^{\text{crit}} v_{m,c}^{\text{crit}} & \text{for } \rho_{m,i}^{\text{efc}}(k) \geq \rho_m^{\text{crit}} \end{cases} \quad (18)$$

$$S_{m,i}(\rho_{m,i}^{\text{efc}}(k)) = \begin{cases} \mu_m \rho_m^{\text{crit}} v_{m,c}^{\text{crit}} & \text{for } \rho_{m,i}^{\text{efc}}(k) < \rho_m^{\text{crit}} \\ \mu_m \rho_{m,i}^{\text{efc}}(k) V_c(\rho_{m,i}^{\text{efc}}(k)) & \text{for } \rho_{m,i}^{\text{efc}}(k) \geq \rho_m^{\text{crit}} \end{cases} \quad (19)$$

For more details about FASTLANE, we refer to [26, 27].

III. TRAFFIC EMISSION MODELS

A. VT-Macro

The VT-macro model [4] is a macroscopic emission and fuel consumption model. It has been developed based on an integration of the VT-micro model [21] and the METANET model. However, it is possible to use the VT-macro model together with other macroscopic traffic flow models. VT-micro is a microscopic emissions and fuel consumption model, i.e., it yields the emissions and fuel consumption rate of an individual vehicle. This model requires the speed and the acceleration of a single vehicle as inputs. However, the METANET model only yields the space-mean speeds of segments. The accelerations can be derived from the METANET model as follows [4].

For each segment, two acceleration components are considered: inter-segment acceleration and cross-segment acceleration. They are defined as follows:

$$a_{m,i}^{\text{inter}}(k) = \frac{v_{m,i}(k) - v_{m,i}(k-1)}{T} \quad (20)$$

$$a_{\alpha,\beta}^{\text{cross}}(k) = \frac{v_{\beta}(k) - v_{\alpha}(k-1)}{T} \quad (21)$$

where the indices α and β represent different adjacent segments, on-ramps, or off-ramps. The numbers of vehicles that correspond to these two accelerations are

$$n_{m,i}^{\text{inter}}(k) = L_m \mu_m \rho_{m,i}(k) - T q_{m,i}(k) \quad (22)$$

$$n_{\alpha,\beta}^{\text{cross}}(k) = T q_{\alpha}(k) \quad (23)$$

Based on the accelerations, the VT-macro model yields the estimates of emission rates and fuel consumption rates of segments:

$$J_{y,m,i}^{\text{inter}}(k) = n_{m,i}^{\text{inter}}(k) \exp \left(\tilde{v}_{m,i}^T(k) P_y \tilde{a}_{m,i}^{\text{inter}}(k) \right) \quad (24)$$

$$J_{y,\alpha,\beta}^{\text{cross}}(k) = n_{\alpha,\beta}^{\text{cross}}(k) \exp \left(\tilde{v}_{\alpha}^T(k) P_y \tilde{a}_{\alpha,\beta}^{\text{cross}}(k) \right) \quad (25)$$

where P_y is a model parameter matrix, $y \in Y = \{\text{CO}, \text{NO}_x, \text{HC}, \text{fuel}\}$, and $\tilde{v}_{m,i}$, $\tilde{a}_{m,i}^{\text{inter}}$, \tilde{v}_{α} , and $\tilde{a}_{\alpha,\beta}^{\text{cross}}$ are vectors in the form of $\tilde{x} = [1 \ x \ x^2 \ x^3]^T$.

The VT-macro model does not yield estimates of the emission rate of CO_2 . According to [28, 29], an approximate affine relationship exists between CO_2 emission rate and fuel consumption rate. Thus, the CO_2 emission rate ($J_{\text{CO}_2,m,i}$) can be estimated through

$$J_{\text{CO}_2,m,i}(k) = \gamma_1 v_{m,i}(k) + \gamma_2 J_{\text{fuel},m,i}(k) \quad (26)$$

where γ_1 and γ_2 are model parameters, and $J_{\text{fuel},m,i}$ is the fuel consumption rate given by

$$J_{\text{fuel},m,i}(k) = J_{\text{fuel},m,i}^{\text{inter}}(k) + \sum_{\alpha \in I_{\text{up}}} J_{\text{fuel},\alpha,(m,i)}^{\text{cross}}(k) \quad (27)$$

where I_{up} is the set that includes all the upstream segments and origins that connect to segment (m,i) .

B. VERSIT+

The VERSIT+ model [22, 23] is a microscopic emission model developed based on a large number of emission tests. It is able to predict emissions at different geographical scales. The VERSIT+ model requires speed-data profile as input. In the latest version of VERSIT+ [23], the emission rate J_y is estimated as follows:

$$J_y(k) = \begin{cases} u_{0,y} & \text{if } v < 5, a < 0.5 \\ u_{1,y} + u_{2,y}z + u_{3,y}(z-1)_+ & \text{if } v < 50 \\ u_{4,y} + u_{5,y}z + u_{6,y}(z-1)_+ & \text{if } 50 < v < 80 \\ u_{7,y} + u_{8,y}(z-0.5)_+ + u_{9,y}(z-1.5)_+ & \text{if } v > 80 \end{cases} \quad (28)$$

where the function $(x)_+$ is defined as follows: $(x)_+ = 0$ for $x < 0$, and $(x)_+ = x$ for $x > 0$, y represents emission categories (e.g. CO_2 , NO_x , and PM_{10}^2), $u_{0,y}, \dots, u_{9,y}$ are model parameters, and z is defined as

$$z = a + 0.014v \quad (29)$$

in which v is the speed of a single vehicle in km/h, and a is the acceleration of a single vehicle in m/s^2 .

IV. NEW TRAFFIC FLOW MODELS

In this paper, we aim to develop online MPC for traffic networks. Considering the trade-off between computation complexity and accuracy, multi-class macroscopic traffic flow models will be adopted. In the ensuing, we represent the new multi-class METANET model and the extensions on FASTLANE.

A. Multi-Class METANET

Based on the method that is used by Logghe for developing the multi-class LWR model [9], we propose a new multi-class METANET model. The new multi-class METANET model is developed based on the following assumptions [9]:

- User optimum: all vehicles try to minimize their travel time, and to maximize their speeds. Vehicle classes are divided over the total road space in such a way that a

²PM10 represents respirable suspended particle in the atmosphere, i.e., particles with diameter of 10 micrometres or less.

vehicle cannot increase its speed without slowing down slower vehicles.

- Optimal road use: it is assumed that a vehicle class never occupies more space than necessary.

In particular, it is assumed that each vehicle class is constrained within an assigned space of the road, being subject to its own fundamental diagram:

$$q_{m,i,c} = \alpha_{m,i,c} Q_c \left(\frac{\rho_{m,i,c}}{\alpha_{m,i,c}} \right) \quad (30)$$

$$(31)$$

where $Q_c(\rho_{m,i,c}) = \mu_m \rho_{m,i,c} v_{m,i,c}$ is the flow function of vehicles of class c , and $\alpha_{m,i,c}$ is the road fraction of vehicle class c defined as the ratio between the assigned space and the whole road space. The road fractions for different classes of vehicles are always positive, with the sum of all fractions limited by 1:

$$\alpha_{m,i,c} \geq 0 \quad (32)$$

$$\sum_{c=1}^{n_c} \alpha_{m,i,c} \leq 1 \quad (33)$$

The class-specific density $\rho_{m,i,c}$, outflow $q_{m,i,c}$, and queue length $w_{o,c}$ are computed through single-class equations (see Section II-A). However, class-dependent parameters ($\tau_{m,c}$, $\eta_{m,c}$, $\kappa_{m,c}$, $\rho_{\text{crit},m,c}$, $v_{\text{free},m,c}$, $a_{m,c}$, and $\delta_{m,c}$) are necessary for computing the speed $v_{m,i,c}$ and the origin flow $q_{o,c}$. These two variables are described through the following equations:

$$\begin{aligned} v_{m,i,c}(k+1) = & v_{m,i,c}(k) + \frac{T}{\tau_{m,c}} \left(V_{m,c} \left(\frac{\rho_{m,i,c}(k)}{\alpha_{m,i,c}(k)} \right) - v_{m,i,c}(k) \right) \\ & + \frac{T}{L_m} v_{m,i,c}(k) (v_{m,i-1,c}(k) - v_{m,i,c}(k)) \\ & - \frac{T \eta_{m,c}}{L_m \tau_{m,c}} \frac{\rho_{m,i+1,c}(k) - \rho_{m,i,c}(k)}{\rho_{m,i,c}(k) + \rho_{\text{crit},m,c} \kappa_{m,c}} \end{aligned} \quad (34)$$

in which

$$\begin{aligned} & V_{m,c} \left(\frac{\rho_{m,i,c}(k)}{\alpha_{m,i,c}(k)} \right) \\ = & v_{\text{free},m,c} \exp \left(\frac{-1}{a_{m,c}} \left(\frac{\rho_{m,i,c}(k)/\alpha_{m,i,c}(k)}{\rho_{\text{crit},m,c}} \right)^{a_{m,c}} \right) \end{aligned} \quad (35)$$

The desired speed with a variable speed limit is

$$\begin{aligned} & V_{m,c} \left(\frac{\rho_{m,i,c}(k)}{\alpha_{m,i,c}(k)} \right) \\ = & \min \left(v_{\text{free},m,c} \exp \left(\frac{-1}{a_{m,c}} \left(\frac{\rho_{m,i,c}(k)/\alpha_{m,i,c}(k)}{\rho_{\text{crit},m,c}} \right)^{a_{m,c}} \right), \right. \\ & \left. (1 + \delta_{m,c}) v_{\text{SL},m,i}(k) \right) \end{aligned} \quad (36)$$

In addition, the outflow of vehicles of class c at origin o is

$$\begin{aligned} q_{o,c}(k) = & \min \left[d_{o,c}(k) + \frac{w_{o,c}(k)}{T}, \alpha_{m,1,c}(k) C_{o,c} r_o(k), \right. \\ & \left. \alpha_{m,1,c}(k) C_{o,c} \left(\frac{\rho_{\text{max},m,c} - \rho_{m,1,c}(k)/\alpha_{m,1,c}(k)}{\rho_{\text{max},m,c} - \rho_{\text{crit},m,c}} \right) \right] \end{aligned} \quad (37)$$

where $d_{o,c}$ is the demand of vehicles of class c at origin o , $\alpha_{m,1,c}$ is the space fraction of vehicle class c in the segment to which the origin o is connected, $C_{o,c}$ is the theoretical maximum capacity of origin o if there would be only vehicles of class c , $\rho_{\text{max},m,c}$ is the theoretical maximum density of the link m that connects to the origin if there would be only vehicles of class c , and $\rho_{m,1,c}$ is the density of vehicles of class c in the segment that connects to the origin.

According to different densities, three traffic regimes are considered here: free flow, congestion, and semi-congestion.

1) *Free-Flow*: In free-flow regime, the density of each vehicle class in its assigned space of the road is less than or equal to the critical density of that class.

The constraint that separates the free-flow regime from the semi-congestion regime is

$$\sum_{c=1}^{n_c} \frac{\rho_{m,i,c}(k)}{\rho_{\text{crit},m,c}} \leq 1 \quad (38)$$

The constraint (38) is derived from (33) and the following sufficient and necessary condition for the free-flow regime:

$$\frac{\rho_{m,i,c}(k)}{\alpha_{m,i,c}(k)} \leq \rho_{\text{crit},m,c} \quad \text{for all } c \quad (39)$$

In order to have all classes of vehicles in the free-flow regime, the relation (39) should hold. According to (38) and (39), we define the space fraction of vehicle class c as

$$\alpha_{m,i,c}(k) = \frac{\rho_{m,i,c}(k)/\rho_{\text{crit},m,c}}{\sum_{j=1}^{n_c} \rho_{m,i,j}(k)/\rho_{\text{crit},m,j}} \quad (40)$$

2) *Semi-Congestion*: In semi-congestion regime, the density of at least one vehicle class in its assigned space of the road is less than or equal to the critical density of that class, and the density of at least one vehicle class in its assigned space of the road is more than the critical density of that class.

The constraint distinguishing semi-congestion from congestion is

$$\sum_{c=1}^{n_c} \frac{\rho_{m,i,c}(k)}{\rho_{\text{crit},m,c}^*} \leq 1 \quad (41)$$

where $\rho_{\text{crit},m,c}^*$ is a parameter for vehicle class c that is determined through the following equation:

$$\rho_{\text{crit},m,c}^* = \rho_{\text{crit},m,c} \left[-a_{m,c} \ln \left(\frac{v_{\text{free},m,c}^*}{v_{\text{free},m,c}} \exp \left(\frac{-1}{a_{m,c}^*} \right) \right) \right]^{\frac{1}{a_{m,c}}} \quad (42)$$

where c_m^* is the vehicle class with the slowest desired speed in free flow: $c_m^* = \arg \min_{c=1, \dots, n_c} (v_{\text{free},m,c} \exp(-1/a_{m,c}))$.

The constraint (41) is obtained by assuming that class c_m^* is on the verge of getting in congested mode, and all the other classes are congested. Also, the desired speed of vehicle class c_m^* is less than or equal to the desired speed of other congested vehicle classes:

$$\begin{aligned} & V_{c_m^*} \left(\frac{\rho_{m,i,c_m^*}(k)}{\alpha_{m,i,c_m^*}(k)} \right) \leq V_c \left(\frac{\rho_{m,i,c}(k)}{\alpha_{m,i,c}(k)} \right) \\ & \text{for } c = 1, \dots, n_c \text{ with } c \neq c_m^* \end{aligned} \quad (43)$$

Based on the assumption of optimal road use, the space fraction of vehicle class c_m^* is chosen as

$$\alpha_{m,i,c_m^*}(k) = \frac{\rho_{m,i,c_m^*}(k)}{\rho_{\text{crit},m,c_m^*}} \quad (44)$$

The constraint (41) is obtained by considering (33), (43), and (44).

Suppose that $S_{m,i,\text{cong}}(k)$ denotes the set of all vehicle classes that are in congested mode in segment i of link m at time step k , and $S_{m,i,\text{free}}(k)$ denotes the set of all vehicle classes that are in free flow in segment i of link m at time step k . The space fractions for the vehicle classes that are in free flow mode are

$$\alpha_{m,i,c} = \frac{\rho_{m,i,c}(k)}{\rho_{\text{crit},m,c}} \quad \text{for } c \in S_{m,i,\text{free}}(k) \quad (45)$$

The space fractions for the congested vehicle classes are obtained through solving the following equation set:

$$\left\{ \begin{array}{l} V_{m,c} \left(\frac{\rho_{m,i,c}(k)}{\alpha_{m,i,c}(k)} \right) = V_{m,l_{m,i}(k)} \left(\frac{\rho_{m,i,l_{m,i}(k)}}{\alpha_{m,i,l_{m,i}(k)}} \right) \\ \text{for } c \in S_{m,i,\text{cong}}(k) / \{l_{m,i}(k)\} \\ \sum_{c \in S_{m,i,\text{cong}}(k)} \alpha_{m,i,c}(k) = 1 - \sum_{\hat{c} \in S_{m,i,\text{free}}(k)} \alpha_{m,i,\hat{c}}(k) \end{array} \right. \quad (46)$$

where $l_{m,i}(k)$ is any element of the set $S_{m,i,\text{cong}}(k)$.

3) *Congestion*: In congestion regime, the density of each vehicle class in its assigned space of the road is more than the critical density of that class; the desired speeds of all classes of vehicles are equal.

The constraint of the congestion regime is the maximum density restriction:

$$\sum_{c=1}^{n_c} \frac{\rho_{m,i,c}(k)}{\rho_{\text{max},m,c}} \leq 1 \quad (47)$$

The fractions can be derived by equating the desired speeds of all classes of vehicles:

$$\left\{ \begin{array}{l} V_1 \left(\frac{\rho_{m,i,1}(k)}{\alpha_{m,i,1}(k)} \right) = V_2 \left(\frac{\rho_{m,i,2}(k)}{\alpha_{m,i,2}(k)} \right) \\ \vdots \\ V_{n_c-1} \left(\frac{\rho_{m,i,n_c-1}(k)}{\alpha_{m,i,n_c-1}(k)} \right) = V_{n_c} \left(\frac{\rho_{m,i,n_c}(k)}{\alpha_{m,i,n_c}(k)} \right) \\ \sum_{c=1}^{n_c} \alpha_{m,i,c}(k) = 1 \end{array} \right. \quad (48)$$

B. Extensions on FASTLANE

The FASTLANE model of [26, 27] does not yield the estimation of queue lengths at origins. Besides, traffic control measures are also not included, such as speed limit and ramp metering. Here we extend the FASTLANE model with a queue length equation, and we also include variable speed limits and ramp metering.

Just as in METANET, we introduce a simple queue equation for estimating the queue lengths at origins:

$$w_{o,c}(k+1) = w_{o,c}(k) + T(d_{o,c}(k) - q_{o,c}(k)) \quad (49)$$

where $w_{o,c}$ is the queue length of vehicles of class c at origin o , $q_{o,c}$ is the outflow of the vehicles of class c at origin o , and $d_{o,c}$ is the demand of the vehicles of class c at origin o .

Following the METANET speed equation of [25] (i.e. (5)), a variable speed limit is incorporated in the speed equation as follows:

$$v_{m,i,c}(k) = \min(V_c(\rho_{m,i}^{\text{efc}}(k)), (1 + \delta_{m,c})v_{\text{SL},m,i}(k)) \quad (50)$$

In order to apply ramp metering in traffic networks, the on-ramp flow equation with a ramp metering is defined as

$$q_{o,(m,1),c}(k) = \frac{1}{\eta_{o,c}(k)} \min \left(r_o(k) D_{o,c}(k), \kappa_o \lambda_{o,c}(k) S_{m,1}(k) \right) \quad (51)$$

in which o indicates the on-ramp, $r_o(k)$ is the ramp metering rate at this on-ramp, $(m, 1)$ indicates the segment to which the on-ramp connects, and κ_o represents the proportion of the supply that is distributed to on-ramp o in the total supply of segment $(m, 1)$.

V. MULTI-CLASS TRAFFIC EMISSION MODELS

Since we want to consider emission reduction in online MPC for traffic networks, multi-class macroscopic emission models are adopted in this paper. In particular, multi-class VT-macro and multi-class VERSIT+ are developed as follows.

A. Multi-Class VT-Macro

The VT-macro model [4] is currently still single-class, and the differences among different vehicle classes are not considered yet. It is necessary to extend the VT-macro model to be multi-class when it is used together with multi-class macroscopic traffic models.

For multi-class traffic flow, the accelerations for each class c are computed through the following equations:

$$a_{m,i,c}^{\text{inter}}(k) = \frac{v_{m,i,c}(k+1) - v_{m,i,c}(k)}{T} \quad (52)$$

$$a_{\alpha,\beta,c}^{\text{cross}}(k) = \frac{v_{\beta,c}(k+1) - v_{\alpha,c}(k)}{T} \quad (53)$$

When the traffic model is FASTLANE, the state variables are equivalent values in pce; the corresponding actual numbers of vehicles are then

$$n_{m,i,c}^{\text{inter}}(k) = \frac{L_1^{\text{veh}}}{L_c^{\text{veh}}} (L_m \mu_m \rho_{m,i,c}(k) - T q_{m,i,c}(k)) \quad (54)$$

$$n_{\alpha,\beta,c}^{\text{cross}}(k) = \frac{L_1^{\text{veh}}}{L_c^{\text{veh}}} T q_{\alpha,c}(k) \quad (55)$$

However, when the traffic model is the newly proposed multi-class METANET, the numbers of vehicles are

$$n_{m,i,c}^{\text{inter}}(k) = L_m \mu_m \rho_{m,i,c}(k) - T q_{m,i,c}(k) \quad (56)$$

$$n_{\alpha,\beta,c}^{\text{cross}}(k) = T q_{\alpha,c}(k) \quad (57)$$

The emission rate for each vehicle class in segment i of link m is

$$J_{y,m,i,c}^{\text{inter}}(k) = n_{m,i,c}^{\text{inter}}(k) \exp \left(\tilde{v}_{m,i,c}^T(k) P_{y,c} \tilde{a}_{m,i,c}^{\text{inter}}(k) \right) \quad (58)$$

$$J_{y,\alpha,\beta,c}^{\text{cross}}(k) = n_{\alpha,\beta,c}^{\text{cross}}(k) \exp \left(\tilde{v}_{\alpha,c}^T(k) P_{y,c} \tilde{a}_{\alpha,\beta,c}^{\text{cross}}(k) \right) \quad (59)$$

in which $P_{y,c}$ is a class-dependent parameter matrix.

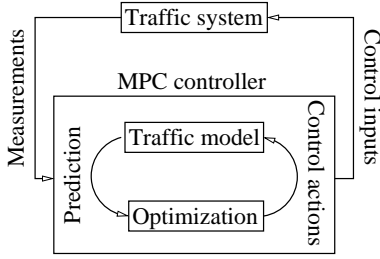


Fig. 1: Closed-loop model predictive control

The CO₂ emission rate for each vehicle class can be estimated through

$$J_{\text{CO}_2,m,i,c}(k) = \gamma_{1,c}v_{m,i,c}(k) + \gamma_{2,c}J_{\text{fuel},m,i,c}(k) \quad (60)$$

where $\gamma_{1,c}$ and $\gamma_{2,c}$ are model parameters, and $J_{\text{fuel},m,i,c}$ is the fuel consumption rate given by

$$J_{\text{fuel},m,i,c}(k) = J_{\text{fuel},m,i,c}^{\text{inter}}(k) + \sum_{\alpha \in I_{\text{up}}} J_{\text{fuel},\alpha,(m,i),c}^{\text{cross}}(k) \quad (61)$$

B. Multi-Class VERSIT+

Similarly to the multi-class VT-macro model, we develop a multi-class VERSIT+ model. The inter-segment/cell acceleration and the cross-segment/cell acceleration are also used here. For segment/cell i of link m , the emission rate of vehicle class c is estimated through substituting speed, inter-segment/cell acceleration, and cross-segment/cell acceleration into (28). For detailed equations, please refer to the Appendix A.

Remark. *The approach that links VERSIT+ to multi-class macroscopic traffic flow models is general in the sense that it can be used for any emission model using car characteristics, and with speed, acceleration, and jerk as inputs. Since the jerk is not derived above, jerk equations are included in Appendix B.*

VI. ONLINE MODEL PREDICTIVE CONTROL FOR TRAFFIC NETWORK

A. Model Predictive Control

We choose Model Predictive Control (MPC) [30] for online traffic management, since it can deal with nonlinear systems, multi-criteria optimization, and constraints. MPC is a control approach based on dynamic prediction and a receding horizon scheme. In MPC, an objective function is used to capture the future performance of the traffic network to be controlled over some prediction horizon. The future performance is obtained through model-based prediction. The controller determines the input sequence that optimizes the value of the objective function. According to the receding horizon scheme, only the first element of this optimal input sequence is applied to the controlled traffic network. The closed-loop MPC approach is shown in Fig. 1.

In this paper, the newly proposed models (FASTLANE, multi-class METANET, multi-class VT-macro, and multi-class VERSIT+) are used as prediction models. The control measures that we choose are variable speed limits and ramp metering.

B. Performance Criteria

Many performance criteria can be considered when conducting the objective function for traffic management. In this paper, we introduce Total Time Spent (TTS) and Total Emissions (TE).

TTS is the total time that all vehicles need to leave the considered traffic network. Here, the TTS is defined as

$$\text{TTS}(k_c) = T \sum_{j=k_c M}^{(k_c+N_p)M-1} \sum_{c=1}^{n_c} p_c \left[\sum_{(m,i) \in I_{\text{all}}} \mu_m \rho_{m,i,c}(j) L_m + \sum_{o \in O_{\text{all}}} w_{o,c}(j) \right] \quad (62)$$

where I_{all} is the set of all pairs of link and segment/cell indices (m, i) in the traffic network, O_{all} is the set of the indices of all origins, k_c is the control time step counter, which corresponds to the time instant $t = k_c T_c$ (T_c : the control time interval), N_p is the prediction horizon, $M = T/T_c$ is assumed to be a positive integer, and $p_c = s_c/s_1$ (s_c : the class-specific gross stopping distance of vehicles of class c) indicates the passenger car equivalents (pce) for vehicles of class c .

TE is the amount of emissions that all vehicles in the traffic network generate before leaving. The TE of emission type y is defined as

$$\text{TE}_y(k_c) = T \sum_{j=k_c M}^{(k_c+N_p)M-1} \sum_{c=1}^{n_c} \left[\sum_{(m,i) \in I_{\text{all}}} J_{y,m,i,c}^{\text{inter}}(j) + \sum_{\alpha, \beta \in P_{\text{all}}} J_{y,\alpha,\beta,c}^{\text{cross}}(j) \right] \quad (63)$$

in which P_{all} is the set of all pairs of adjacent cells.

C. End-Point Penalties

In MPC for traffic network, satisfying control performance may lead to long prediction horizon, since the prediction horizon is in the order of the typical travel time for a vehicle to cross the traffic network [25]. This makes computation slow and complex for large-scale traffic networks. For obtaining satisfying performance without increasing the prediction horizon too much, we propose to use end-point penalties to distinguish vehicles that are at different positions in the controlled traffic network. In order to bring as many vehicles as close as possible to their destination, vehicles that are further from their destinations need more attention. Hence, terms with different values corresponding to vehicles with different distances to their destinations should be included in the objective function. We develop these terms and call them end-point penalties.

1) *End-Point Penalty Derived from TTS*: One way to represent the differences among vehicles with different distances to their destinations is to use the different times needed for them to arrive to their destinations. The end-point penalty is then defined as the number of vehicles in each segment/cell multiplied by the time $t_{m,i,c}^{\text{rem}}((k_c + N_p)M)$ that a vehicle that is present in that segment/cell at time step $(k_c + N_p)M$ would on the average need to get to its destination. For vehicles in queues, the end-point penalty is defined as the number of vehicles in each queue multiplied

by the time $t_{o,c}^{\text{rem}}((k_c + N_p)M)$ that a vehicle present in that queue at time step $(k_c + N_p)M$ would on the average need to get to its destination. This yields an estimate of the total time spent for all vehicles that are still in the network at time step $(k_c + N_p)M$:

$$\begin{aligned} \text{TTS}^{\text{end-point}}(k_c) = & \\ & \sum_{c=1}^{n_c} \sum_{(m,i) \in I_{\text{all}}} \mu_m \rho_{m,i,c}((k_c + N_p)M) L_m t_{m,i,c}^{\text{rem}}((k_c + N_p)M) \\ & + \sum_{o \in O_{\text{all}}} w_{o,c}((k_c + N_p)M) t_{o,c}^{\text{rem}}((k_c + N_p)M) \quad (64) \end{aligned}$$

2) *End-Point Penalty Derived from TE*: Another way to represent the differences among vehicles with different distances to their destinations is to use the different emissions generated by them. The end-point penalty is then defined as the number of vehicles in each segment/cell at time step $(k_c + N_p)M$ multiplied by the emissions $\text{TE}_{y,m,i,c}^{\text{rem}}((k_c + N_p)M)$ that a vehicle that is present in that segment/cell at time step $(k_c + N_p)M$ would on the average generate before leaving the network. For vehicles in queues, the end-point penalty is defined as the number of vehicles in each queue at time step $(k_c + N_p)M$ multiplied by the emissions $\text{TE}_{y,o,c}^{\text{rem}}((k_c + N_p)M)$ that a vehicle that is present in that queue at time step $(k_c + N_p)M$ would on the average generate before leaving the network. This yields the estimate of the total emissions that the remaining vehicles at time step $(k_c + N_p)M$ generate before leaving the network:

$$\begin{aligned} \text{TE}_y^{\text{end-point}}(k_c) = & \\ & \sum_{c=1}^{n_c} \sum_{(m,i) \in I_{\text{all}}} L_m \rho_{m,i,c}((k_c + N_p)M) \mu_m \text{TE}_{y,m,i,c}^{\text{rem}}((k_c + N_p)M) \\ & + w_{o,c}((k_c + N_p)M) \text{TE}_{y,o,c}^{\text{rem}}((k_c + N_p)M) \quad (65) \end{aligned}$$

D. Overall Objective Function

For different traffic conditions, the traffic control objectives may be conflicting [31]. We aim to achieve a balanced trade-off between TTS and TE here. However, the approach that we develop is generic, and it can also accommodate other performance indicators.

The overall objective function of the online traffic control in this paper is defined as follows:

$$\begin{aligned} J(k_c) = & \xi_{\text{TTS}} \frac{\text{TTS}(k_c)}{\text{TTS}_{\text{nom}}} + \sum_{y \in Y} \xi_{\text{TE},y} \frac{\text{TE}_y(k_c)}{\text{TE}_{y,\text{nom}}} \\ & + \frac{\xi_{\text{ramp}}}{N_c N_{\text{RM}}} \sum_{l=k_c}^{k_c + N_c - 1} \sum_{o \in O_{\text{ramp}}} (r_{\text{ctrl},o}(l) - r_{\text{ctrl},o}(l-1))^2 \\ & + \frac{\xi_{\text{speed}}}{N_c N_{\text{VSL}}} \sum_{l=k_c}^{k_c + N_c - 1} \sum_{(m,i) \in I_{\text{speed}}} \left(\frac{v_{\text{ctrl},m,i}(l) - v_{\text{ctrl},m,i}(l-1)}{v_{\text{free},m,\text{max}}} \right)^2 \\ & + \xi_{\text{TTS}}^{\text{end-point}} \frac{\text{TTS}^{\text{end-point}}(k_c)}{\text{TTS}_{\text{nom}}^{\text{end-point}}} \\ & + \sum_{y \in Y} \xi_{\text{TE},y}^{\text{end-point}} \frac{\text{TE}_y^{\text{end-point}}(k_c)}{\text{TE}_{y,\text{nom}}^{\text{end-point}}} \quad (66) \end{aligned}$$

where the third and fourth terms of (66) are penalties to avoid abrupt variations in control inputs, O_{ramp} is the set of

all the metered on-ramps, $r_{\text{ctrl},o}$ is the ramp metering rate of on-ramp o corresponding to control time steps ($t = k_c T_c$), I_{speed} is the set of all segments/cells with speed limits, $v_{\text{ctrl},m,i}$ is the speed limit in segment/cell i of link m corresponding to control time steps ($t = k_c T_c$), and $v_{\text{free},m,\text{max}} = \max_c v_{m,c}^{\text{free}}$ is the maximum free-flow speed of all vehicle classes. Moreover, ξ_{TTS} , $\xi_{\text{TE},y}$, ξ_{ramp} , ξ_{speed} , $\xi_{\text{TTS}}^{\text{end-point}}$, and $\xi_{\text{TE},y}^{\text{end-point}}$ are nonnegative weights, TTS_{nom} , $\text{TE}_{y,\text{nom}}$, $\text{TTS}_{\text{nom}}^{\text{end-point}}$, and $\text{TE}_{y,\text{nom}}^{\text{end-point}}$ are the corresponding 'nominal' values for some nominal control profile (here we take the 'nominal' control profile as no-control case), N_{RM} is the number of groups of metered on-ramps, and N_{VSL} is the number of groups of variable speed limits.

VII. BENCHMARK EXPERIMENT

A. Benchmark Network

The simulation experiment is based on the Dutch freeway A13, where we consider the direction from Den Haag to Rotterdam, as shown in Fig. 2. The upstream of A13 is considered to be the origin (O_0) of the considered stretch, and the downstream of A13 is considered to be the destination (D_0) of the considered stretch. The main road subsumes three lanes, and variable speed limits are equipped through the whole stretch. There are four on-ramps (O_1 , O_2 , O_3 , and O_4) and four off-ramps (O_5 , O_6 , O_7 , and O_8) which contain single lane. All the on-ramps are metered. According to the location of on-ramps, off-ramps, and speed limits, the main road (7.8 km) is divided into 21 links, and in total 23 segments, i.e., most links only have 1 segment.

The microscopic simulators VISSIM and Enviver are used for representing the real traffic network. VISSIM is used for simulating the traffic flows, and Enviver is used for simulating the emissions. The developed multi-class traffic flow and emission models are used as prediction models. In both the process models and the prediction models, we consider two classes of vehicles (i.e. cars and trucks). The closed-loop control procedure is shown in Fig. 3.

B. Parameter Identification

In order to describe the traffic flows and emissions through the models developed in Sections IV and V, the parameters for these models need to be calibrated. The mainstream demand and the on-ramp demands for identification, which are shown in Fig. 4, are generated based on field measurements of the A13 on Feb. 18, 2014. The fraction of trucks in all the demands is taken as 0.1, considering the actual situation in A13. For multi-class METANET and FASTLANE, the objective for the identification procedure is TTS. Similarly, for multi-class VERSIT+ and multi-class VT-macro, the objective for the identification procedure is TE, and only CO_2 is considered.

The prediction horizon length is chosen as 15 minutes, which is about the average time needed for a vehicle to leave the network. For control period from 8.00 to 10.00, the average validation errors within the prediction horizon between the measured TTS and the predicted TTS by

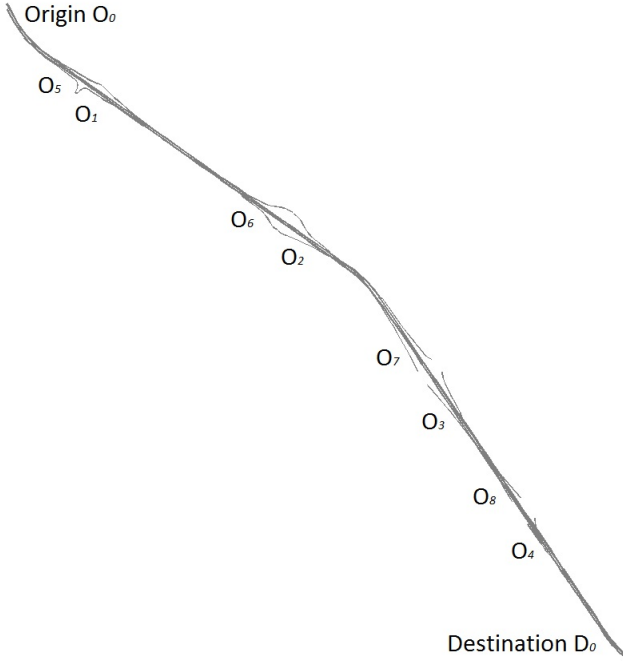


Fig. 2: Dutch Freeway A13

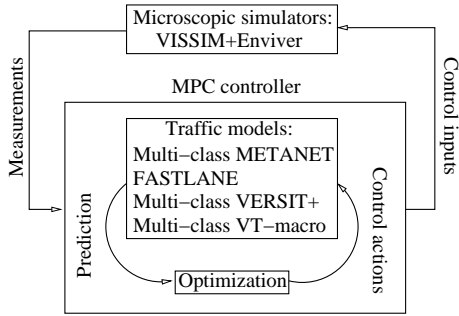


Fig. 3: Closed-loop model predictive control for A13

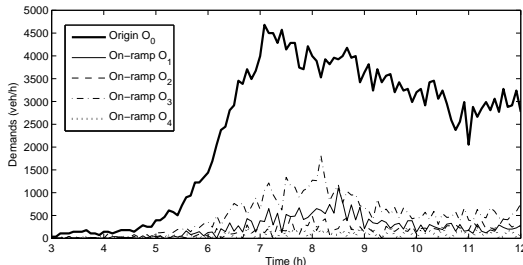


Fig. 4: Demands for A13

Table 1 Validation errors for traffic flow models

	Scenario 1	Scenario 2	Scenario 3
Multi-class METANET	10.0%	11.5%	12.0%
FASTLANE	8.7%	10.4%	10.6%

Table 2 Validation errors for emission models

	Scenario 1	Scenario 2	Scenario 3
Multi-class VERSIT+	1.6%	2.4%	5.6%
Multi-class VT-macro	4.0%	2.5%	3.4%

METANET and FASTLANE are shown in Table 1. Three scenarios are considered for validation here:

- Scenario 1: the scenario used for identification;
- Scenario 2: Scenario 1 + sinusoidal noise (Amplitude: 5% of the demands for Scenario 1, cycle time: 15 minutes);
- Scenario 3: Scenario 1 + white noise (Amplitude: 5% of the demands for Scenario 1).

The validation errors for multi-class VT-macro and multi-class VERSIT+ in the control period from 8.00 to 10.00 are shown in Table 2.

C. Control Settings

Scenario 1 (as shown in Fig. 3) is considered for control in this case study. The control time interval (T_c) is chosen as 5 minutes, the control horizon (N_c) is chosen as 10 minutes, and the prediction horizon (N_p) is chosen as 15 minutes. The simulation time step (T) is selected to be 6 seconds, according to the length of segments.

We suppose that all the four on-ramps are metered ($N_{RM} = 4$). According to the actual length of the on-ramps, the maximum permitted queue lengths (w_o^{\max} , $o \in O_{\text{ramp}} = \{O_1, O_2, O_3, O_4\}$) are repetitively 100, 100, 200, 50 pce. There are 16 Variable Speed Limits (VSL), which are divided into 4 groups as follows ($N_{VSL} = 4$):

- VSL group 1: the variable speed limits before the first on-ramp, i.e. VSLs 1-4;
- VSL group 2: the variable speed limits between the first on-ramp and the second on-ramp, i.e. VSLs 5-7;
- VSL group 3: the variable speed limits between the second on-ramp and the third on-ramp, i.e. VSLs 8-10;
- VSL group 4: the variable speed limits After the third on-ramp, i.e. VSLs 11-16.

The multi-class models developed in this research are used as prediction models for MPC. Two groups of approaches are implemented for comparing multi-class models and for investigating end-point penalties.

1) *Comparison for multi-class models:* For the multi-class models, we compare four approaches without end-point penalties as follows:

- Approach A: Multi-class METANET and multi-class VERSIT+ without end-point penalties;
- Approach B: Multi-class METANET and multi-class VT-macro without end-point penalties;
- Approach C: FASTLANE and multi-class VERSIT+ without end-point penalties;
- Approach D: FASTLANE and multi-class VT-macro without end-point penalties;

For each approach, we consider 3 combinations of weights without end-point penalties:

- Combination 1: $\xi_{TTS}=1$, $\xi_{TE,y}=0.1$, $\xi_{TTS}^{\text{end-point}}=0$, and $\xi_{TE,y}^{\text{end-point}}=0$;
- Combination 2: $\xi_{TTS}=0.5$, $\xi_{TE,y}=0.5$, $\xi_{TTS}^{\text{end-point}}=0$, and $\xi_{TE,y}^{\text{end-point}}=0$;
- Combination 3: $\xi_{TTS}=0.1$, $\xi_{TE,y}=1$, $\xi_{TTS}^{\text{end-point}}=0$, and $\xi_{TE,y}^{\text{end-point}}=0$.

2) *Comparison for end-point penalties*: In order to show the effects of end-point penalties, we also implement the following four approaches:

- Approach E: Multi-class METANET and multi-class VERSIT+ with end-point penalties;
- Approach F: Multi-class METANET and multi-class VT-macro with end-point penalties;
- Approach G: FASTLANE and multi-class VERSIT+ with end-point penalties;
- Approach H: FASTLANE and multi-class VT-macro with end-point penalties;

Combination 1 ($\xi_{TTS}=1$ and $\xi_{TE,y}=0.1$) is chosen as an example, and for this case an investigation has been done to find appropriate $\xi_{TTS}^{\text{end-point}}$ and $\xi_{TE,y}^{\text{end-point}}$ for end-point penalties, and the values obtained are $\xi_{TTS}^{\text{end-point}}=0.5$ and $\xi_{TE,y}^{\text{end-point}}=0.05$.

We solve the control problem with sequential quadratic programming based on a multi-starting points scheme. An investigation has been done to ensure that the CPU time for the approaches including multi-class METANET and the approaches including FASTLANE are roughly the same. Thus for Approaches A, B, E, and F, 50 starting points are used, and for C, D, G, and H, 70 starting points are used.

D. Results and Analysis

For each approach and each combination of weights, 10 runs with different random seeds are implemented, and the average results are included in the Tables 3-6. In these tables, $J_{\text{improve}}^{\text{TTS,TE}}$ represents the improvement of $\xi_{TTS} \frac{\text{TTS}(k_c)}{\text{TTS}_{\text{nom}}} + \xi_{TE,y} \frac{\text{TE}_y(k_c)}{\text{TE}_{y,\text{nom}}}$ in the entire simulation period w.r.t. the case without control. We define a total objective function J_{total} as follows:

$$J_{\text{total}} = \xi_{TTS} \frac{\text{TTS}(k_c)}{\text{TTS}_{\text{nom}}} + \xi_{TE,y} \frac{\text{TE}_y(k_c)}{\text{TE}_{y,\text{nom}}} + \xi_{\text{queue}} \max_{o \in O_{\text{ramp}}} \frac{\max_{k=1}^{k_{\text{end}}} [\sum_{c=1}^{n_c} P_c w_{o,c}(k)] - w_o^{\text{max}}}{w_o^{\text{max}}} \quad (67)$$

where k_{end} is the last sampling time step of the entire simulation period, and w_o^{max} is the maximum permitted queue length for on-ramp o . The last term of J_{total} represents the maximum queue length constraint violation for all on-ramps, and the weight for this term is set to be a large value: $\xi_{\text{queue}} = 10$. This total objective function is used for comparing the total performance including TTS, TE, and queue length constraint violations, where higher values indicate a worse total performance.

Table 3 Simulation results for Combination 1

Approaches	$J_{\text{improve}}^{\text{TTS,TE}}$	Constraint violations				J_{total}
		O_1	O_2	O_3	O_4	
A	4.4%	5.0%	0%	0%	0%	9.3
B	4.1%	4.7%	0%	0%	0%	9.3
C	2.7%	29.1%	0%	123.6%	0%	21.3
D	-0.4%	43.2%	4.6%	160.7%	0%	25.3

Table 4 Simulation results for Combination 2

Approaches	$J_{\text{improve}}^{\text{TTS,TE}}$	Constraint violations				J_{total}
		O_1	O_2	O_3	O_4	
A	4.3%	6.0%	0%	0%	0%	8.4
B	3.6%	0%	0%	0%	0%	7.9
C	4.9%	19.6%	0%	72.4%	0%	15.0
D	2.5%	100.5%	6.1%	127.5%	0%	20.7

Table 5 Simulation results for Combination 3

Approaches	$J_{\text{improve}}^{\text{TTS,TE}}$	Constraint violations				J_{total}
		O_1	O_2	O_3	O_4	
A	5.1%	6.8%	0%	0%	0%	8.4
B	3.5%	0.1%	0%	0%	0%	7.9
C	11.1%	15.2%	3.2%	63.9%	0%	14.0
D	11.1%	69.7%	0%	160.9%	0%	23.8

Table 6 Simulation results for Combination 1 with end-point penalties

Approaches	$J_{\text{improve}}^{\text{TTS,TE}}$	Constraint violations				J_{total}
		O_1	O_2	O_3	O_4	
E	6.6%	5.1%	0%	0%	0%	9.1
F	4.9%	1.5%	0%	0%	0%	8.9
G	2.1%	50.8%	4.5%	200.7%	0%	29.1
H	2.4%	23.7%	6.7%	168.4%	0%	25.8

1) *Results for multi-class models without end-point penalties*: The results for comparing multi-class models are listed in Tables 3-5. We first focus on the approaches based on multi-class METANET (A and B). According to Tables 3-5, they can all improve the performance for TTS and TE (3.5%-5.1%) w.r.t. the non-control case with relatively small queue length constraint violations (0%-6.8%). Comparing the approach based on multi-class VERSIT+ (A) with the approach based on multi-class VT-macro (B), the values of J_{total} are the same for multi-class VERSIT+ and multi-class VT-macro for Combination 1, and the values of J_{total} for multi-class VERSIT+ are slightly higher than multi-class VT-macro for Combinations 2 and 3. More specifically, the performance improvements for multi-class VERSIT+ are higher than multi-class VT-macro for all combinations of weights. However, the constraint violations for multi-class VERSIT+ are also higher than multi-class VT-macro. This is probably due to the mismatches between the prediction models and the process models.

The approaches based on FASTLANE (C and D) can also improve the performance for TTS and TE w.r.t. the non-control case. Note, however, that for these approaches based on FASTLANE (C and D) there are consistent large queue length constraint violations for on-ramps O_1 (15.2%-100.5%) and O_3 (63.9%-160.9%). Thus the values of J_{total} for FASTLANE (14.0-25.3) are much higher than multi-class METANET (7.9-9.3), and the total performance for approaches based on FASTLANE (C and D) is worse than that of the approaches based on multi-class METANET (A and B).

High constraint violations can lead to traffic jams upstream of the given on-ramps, which is an important issue to be handled when a control approach is developed. According to

the results we obtained for the settings of our experiment, the approaches based on multi-class METANET are more capable of dealing with the queue length constraints.

2) *Results for end-point penalties:* The results for approaches with end-point penalties are included in Table 6, and these results are now compared with results of Table 3. In comparison with the approaches based on multi-class METANET without end-point penalties (A and B in Combination 1), including end-point penalties (E and F) can further improve the performance for TTS and TE (4.9%-6.6%), while the constraint violations (1.5%-5.1%) are still relatively small. In addition, the values of J_{total} (8.9-9.1) are also further reduced w.r.t. the approaches without end-point penalties. Thus, for approaches based on the multi-class METANET we can say that end-point penalties can improve both the performance for TTS and TE and the total performance.

The approaches based on FASTLANE with end-point penalties (G and H) cannot reduce the high constraint violations for on-ramps O_1 (23.7%-50.8%) and O_3 (168.4%-200.7%), and the values of J_{total} (25.8-29.1) increase w.r.t. the corresponding approaches without end-point penalties (C and D). This might be because of the first-order characteristics of FASTLANE, which makes the estimations of end-point penalties less reliable.

VIII. CONCLUSIONS AND FUTURE WORK

In this paper, we have developed a second-order multi-class traffic flow model (multi-class METANET) and two multi-class traffic emission models (multi-class VERSIT+ and multi-class VT-macro). We have also incorporated variable speed limits and ramp metering in the first-order traffic flow model FASTLANE, to allow comparison with multi-class METANET for online Model Predictive Control (MPC) for freeway networks. In contrast to single-class homogeneous models, in these multi-class models the differences among different classes of vehicles (e.g. cars and trucks) are taken into account. End-point penalties are proposed to account for the future extension of the traffic system beyond the prediction horizon.

A benchmark simulation experiment has been implemented to compare these multi-class models. For the prediction models for MPC, eight approaches are considered, i.e., the four combinations of the multi-class traffic flow models and the multi-class traffic emission models, also these combinations with end-point penalties. The results show that the approaches based on multi-class METANET can improve the performance for TTS and TE w.r.t. the non-control case with relatively small constraint violations, and including end-point penalties can further improve the performance for TTS and TE and the total performance. However, the approaches based on FASTLANE lead to consistent queue length constraint violations, which may cause traffic jams upstream the corresponding on-ramps. Furthermore, for these approaches including end-point penalties cannot improve the total performance, probably due to the less reliable estimations of end-point penalties.

For future research, larger networks and more traffic scenarios can be investigated for validating the effectiveness of the proposed multi-class traffic flow and emission models. The impact of end-point penalties can also be further investigated by testing suitable weights for these penalties in different control conditions.

ACKNOWLEDGMENTS

Research supported by the China Scholarship Council and the European COST Action TU1102. In addition, we thank Goof van de Weg (Civil Engineering and Geosciences, Delft University of Technology) for providing the network A13 in VISSIM, which is investigated in the case study of this research.

APPENDIX A EQUATIONS OF MULTI-CLASS VERSIT+

According to Section III-B, Section V-A and Section V-B, the emission rate of vehicles of class c in segment/cell i of link m , is estimated as follows:

$$J_{y,m,i,c}^{\text{inter}} = n_{m,i,c}^{\text{inter}}(k) \begin{cases} u_{0,y,m,i,c} & \text{if } v_{m,i,c} < 5, a_{m,i,c}^{\text{inter}} < 0.5 \\ u_{1,y,m,i,c} + u_{2,y,m,i,c} z_{m,i,c}^{\text{inter},+} \\ + u_{3,y,m,i,c} (z_{m,i,c}^{\text{inter}} - 1)_+ & \text{if } v_{m,i,c} < 50 \\ u_{4,y,m,i,c} + u_{5,y,m,i,c} z_{m,i,c}^{\text{inter},+} \\ + u_{6,y,m,i,c} (z_{m,i,c}^{\text{inter}} - 1)_+ & \text{if } 50 < v_{m,i,c} < 80 \\ u_{7,y,m,i,c} + u_{8,y,m,i,c} (z_{m,i,c}^{\text{inter}} - 0.5)_+ \\ + u_{9,y,m,i,c} (z_{m,i,c}^{\text{inter}} - 1.5)_+ & \text{if } 80 < v_{m,i,c} \end{cases} \quad (68)$$

with

$$z_{m,i,c}^{\text{inter}} = a_{m,i,c}^{\text{inter}} + 0.014 v_{m,i,c} \quad (69)$$

$$J_{y,\alpha,\beta,c}^{\text{cross}} = n_{\alpha,\beta,c}^{\text{cross}}(k) \begin{cases} u_{0,y,\alpha,\beta,c} & \text{if } v_{\alpha,c} < 5, a_{\alpha,\beta,c}^{\text{cross}} < 0.5 \\ u_{1,y,\alpha,\beta,c} + u_{2,y,\alpha,\beta,c} z_{\alpha,\beta,c}^{\text{cross}} \\ + u_{3,y,\alpha,\beta,c} (z_{\alpha,\beta,c}^{\text{cross}} - 1)_+ & \text{if } v_{\alpha,c} < 50 \\ u_{4,y,\alpha,\beta,c} + u_{5,y,\alpha,\beta,c} z_{\alpha,\beta,c}^{\text{cross}} \\ + u_{6,y,\alpha,\beta,c} (z_{\alpha,\beta,c}^{\text{cross}} - 1)_+ & \text{if } 50 < v_{\alpha,c} < 80 \\ u_{7,y,\alpha,\beta,c} + u_{8,y,\alpha,\beta,c} (z_{\alpha,\beta,c}^{\text{cross}} - 0.5)_+ \\ + u_{9,y,\alpha,\beta,c} (z_{\alpha,\beta,c}^{\text{cross}} - 1.5)_+ & \text{if } 80 < v_{\alpha,c} \end{cases} \quad (70)$$

with

$$z_{\alpha,\beta,c}^{\text{cross}} = a_{\alpha,\beta,c}^{\text{cross}} + 0.014 v_{\alpha,c} \quad (71)$$

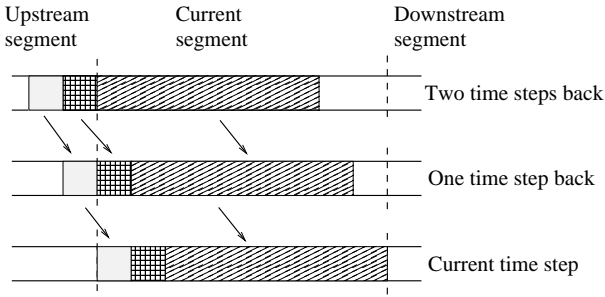


Fig. 5: Jerk: derivative of acceleration

APPENDIX B

COMPUTATION OF JERK FOR MULTI-CLASS TRAFFIC FLOW MODELS

As shown in Fig. 5, there are three kinds of jerks (i.e. derivatives of accelerations) in segment/cell i of link m at time step k :

- Segment $i-1 \rightarrow$ segment $i-1 \rightarrow$ segment i : this kind of jerk corresponds to those vehicles moving within segment $i-1$ from time step $k-2$ to $k-1$, and moving from segment $i-1$ to i from time step $k-1$ to k :

$$\begin{aligned} j_{m,i,c,1}(k) &= \frac{a_{(m,i-1),(m,i),c}^{\text{cross}}(k) - a_{m,i-1,c}^{\text{inter}}(k-1)}{T} \\ &= \frac{v_{m,i,c}(k) - 2v_{m,i-1,c}(k-1) + v_{m,i-1,c}(k-2)}{T^2} \end{aligned} \quad (72)$$

- Segment $i-1 \rightarrow$ segment $i \rightarrow$ segment i : this kind of jerk corresponds to those vehicles moving from segment $i-1$ to i from time step $k-2$ to $k-1$, and moving within segment i from $k-1$ to k :

$$\begin{aligned} j_{m,i,c,2}(k) &= \frac{a_{m,i,c}^{\text{inter}}(k) - a_{(m,i-1),(m,i),c}^{\text{cross}}(k-1)}{T} \\ &= \frac{v_{m,i,c}(k) - 2v_{m,i,c}(k-1) + v_{m,i-1,c}(k-2)}{T^2} \end{aligned} \quad (73)$$

- Segment $i \rightarrow$ segment $i \rightarrow$ segment i : this kind of jerk corresponds to those vehicles moving within segment i from time step $k-2$ to $k-1$, i.e.

$$\begin{aligned} j_{m,i,c,3}(k) &= \frac{a_{m,i,c}^{\text{inter}}(k) - a_{m,i,c}^{\text{inter}}(k-1)}{T} \\ &= \frac{v_{m,i,c}(k) - 2v_{m,i,c}(k-1) + v_{m,i,c}(k-2)}{T^2} \end{aligned} \quad (74)$$

REFERENCES

- [1] C. Caligaris, S. Sacone, and S. Siri. Multi-class freeway traffic: Model predictive control and microscopic simulation. In *Proceedings of the 16th Mediterranean Conference on Control and Automation*, pages 1862–1867, Ajaccio, France, 2008.
- [2] K. Aboudolas, M. Papageorgiou, A. Kouvelas, and E. Kosmatopoulos. A rolling-horizon quadratic-programming approach to the signal control problem in large-scale congested urban road networks. *Transportation Research Part C*, 18(5):680–694, 2010.
- [3] A. Ciskós and I. Varga. Real-time modeling and control objective analysis of motorway emissions. In *Proceedings of the 15th Edition of the Euro Working Group on Transportation*, Paris, France, September 2012.
- [4] S. K. Zegeye, B. De Schutter, H. Hellendoorn, E. Breunese, and A. Hegyi. A predictive traffic controller for sustainable mobility using parameterized control policies. *IEEE Transactions on Intelligent Transportation Systems*, 13(3):1420–1429, September 2012.
- [5] M. Hadiuzzaman and T. Z. Qiu. Cell transmission model based variable speed limit control for freeways. *Canadian Journal of Civil Engineering*, 40(1):46–56, 2013.
- [6] G. C. K. Wong and S. C. Wong. A multi-class traffic flow model - an extension of LWR model with heterogeneous drivers. *Transportation Research Part A*, 36:827–841, 2003.
- [7] M. J. Lighthill and G. B. Whitham. On kinematic waves. II. A theory of traffic flow on long crowded roads. *Proceedings of the Royal Society of London. Series A. Mathematical and Physical Sciences*, 229:317–345, 1955.
- [8] P. I. Richards. Shock waves on the highway. *Operations Research*, 4:42–51, 1956.
- [9] S. Logghe. *Dynamic Modeling of Heterogeneous Vehicular Traffic*. PhD thesis, University of Leuven, Heverlee, Belgium, 2003.
- [10] J. W. C. van Lint, S. P. Hoogendoorn, and M. Schreuder. Fastlane: New multi-class first-order traffic flow model. *Transportation Research Record*, (1):177–187, 2008.
- [11] M. Papageorgiou. *Applications of Automatic Control Concepts to Traffic Flow Modeling and Control*. Lecture Notes in Control and Information Sciences. Springer-Verlag, Berlin, Germany, 1983.
- [12] P. Deo, B. De Schutter, and A. Hegyi. Model predictive control for multi-class traffic flows. In *Proceedings of the 12th IFAC Symposium on Transportation Systems*, pages 25–30, Redondo Beach, California, USA, September 2009.
- [13] A. Messmer and M. Papageorgiou. METANET: A macroscopic simulation program for motorway networks. *Traffic Engineering and Control*, 31(9):466–470, 1990.
- [14] A. Kotsialos and M. Papageorgiou. Traffic flow modeling of large-scale motorway networks using the macroscopic modeling tool METANET. *IEEE Transactions on Intelligent Transportation Systems*, 3(4):282–292, December 2002.
- [15] C. F. Daganzo. Requiem for second-order fluid approximations of traffic flow. *Transportation Research Part B*, 29B(4):277–286, 1995.
- [16] M. Papageorgiou. Some remarks on macroscopic traffic flow modeling. *Transportation Research Part A*, 32(5):323–329, 1998.
- [17] D. Helbing and A. Johansson. On the controversy around Daganzo’s requiem for and Aw-Rascles resurrection of

second-order traffic flow models. *The European Physical Journal B*, 69(4):549–562, 2009.

- [18] T. I. Zachariadis and Z. C. Samaras. An integrated modeling system for the estimation of motor vehicle emissions. *Air and Waste Management Association*, 49:1010–1025, 1999.
- [19] R. M. Corvalan, M. Osses, and C. M. Urrutia. Hot emission model for mobile sources: Application to the metropolitan region of the city of Santiago, Chile. *Air and Waste Management*, 52(2):167–174, 2002.
- [20] M. Zalinger, T. L. Ahn, and S. Hausberger. Improving an instantaneous emission model for passenger cars. In *Proceedings of the 14th Symposium on Transport and Air Pollution*, pages 167–176, Graz, Austria, 2005.
- [21] K. Ahn, A. Trani, H. Rakha, and M. Van Aerde. Microscopic fuel consumption and emission models. In *Proceedings of the 78th Annual Meeting of the Transportation Research Board*, Washington DC, USA, January 1999.
- [22] R. Smit, R. Smokers, and E. Schoen. VERSIT+ LD: Development of a new emission factor model for passenger cars linking real-world emissions to driving cycle characteristics. In *Proceedings of the 14th Symposium on Transport and Air Pollution*, pages 177–186, Graz, Austria, 2005.
- [23] N. E. Ligterink, R. De Lange, and E. Schoen. Refined vehicle and driving-behavior dependencies in the VERSIT+ emission model. In *Proceedings of the ETAPP Symposium*, pages 177–186, Toulouse, France, 2009.
- [24] R. Smit, R. Smokers, and E. Rabe. A new modeling approach for road traffic emissions: VERSIT+. *Transportation Research Part D*, 12:414–422, 2007.
- [25] A. Hegyi, B. De Schutter, and H. Hellendoorn. Model predictive control for optimal coordination of ramp metering and variable speed limits. *Transportation Research Part C*, 13(3):185–209, June 2005.
- [26] J. W. C. van Lint, S. P. Hoogendoorn, and M. Schreuder. Fastlane: New multi-class first-order traffic flow model. *Transportation Research Record*, 2088(1):177–187, 2008.
- [27] J. W. C. van Lint, S. P. Hoogendoorn, and A. Hegyi. Model predictive control for multi-class traffic flows. In *Proceedings of the 12th IFAC Symposium on Transportation Systems*, pages 25–30, Redondo Beach, California, USA, September 2009.
- [28] S. K. Zegeye. *Model-Based Traffic Control for Sustainable Mobility*. PhD thesis, Delft University of Technology, The Netherlands, October 2011.
- [29] M. T. Oliver-Hoyo and G. Pinto. Using the relationship between vehicle fuel consumption and CO₂ emissions to illustrate chemical principles. *Chemical Education*, 85(2):218–220, February 2008.
- [30] E. F. Camacho and C. Bordons. *Model Predictive Control in the Process Industry*. Springer-Verlag, Berlin, Germany, 1995.
- [31] K. Ahn and H. Rakha. The effects of route choice decisions on vehicle energy consumption and emissions. *Transportation Research Part D*, 13(3):151–167, May

2008.



Shuai Liu received the MSc degree in Aeronautical and Astronautical Science and Technology in December, 2011, at National University of Defense Technology, China. She is currently a PhD candidate at the Delft Center for Systems and Control of Delft University of Technology, The Netherlands. Her current research interests are modeling for freeway networks, and robust and distributed control for freeway networks.



Hans Hellendoorn obtained the PhD degree in 1990 on the topic “Reasoning with Fuzzy Logic.”. Next, he started in 1991 at the Siemens Research Laboratory in Munich in the fuzzy control group that he led until 1997. From 1997 to 2000 he was department head for training simulation at Siemens in The Netherlands, and since 2001 he was responsible for innovation management. From 1998 on, he was part-time professor for control theory at University of Technology, Delft. Since 2009 he is full-time professor for control theory at Delft University of Technology in Delft, The Netherlands.

Hans Hellendoorn has written several books and a large number of publications on computational intelligence and control. He currently works on traffic management and control.



Bart De Schutter (IEEE member since 2008, senior member since 2010) received the PhD degree in Applied Sciences (summa cum laude with congratulations of the examination jury) in 1996, at K.U.Leuven, Belgium. Currently, he is a full professor at the Delft Center for Systems and Control of Delft University of Technology in Delft, The Netherlands.

Bart De Schutter is associate editor of the IEEE Transactions on Intelligent Transportation Systems and of Automatica. His current research interests include control of discrete-event and hybrid systems, multi-level and distributed control, and intelligent transportation and infrastructure systems.